

Imitation and Transfer Q-Learning-Based Parameter Identification for Composite Load Modeling

Jian Xie, *Student Member, IEEE*, Zixiao Ma¹, *Graduate Student Member, IEEE*,
 Kaveh Dehghanpour², *Member, IEEE*, Zhaoyu Wang², *Member, IEEE*, Yishen Wang², *Member, IEEE*,
 Ruisheng Diao³, *Senior Member, IEEE*, and Di Shi³, *Senior Member, IEEE*

AQ1

Abstract—Fast and accurate load parameter identification has a large impact on power systems operation and stability analysis. This article proposes a novel Imitation and Transfer Q-learning (ITQ)-based method to identify parameters of composite constant impedance-current-power (ZIP) and induction motor (IM) load models. Firstly, an imitation learning process is introduced to improve the exploitation and exploration processes. Then, a transfer learning method is employed to overcome the challenge of time-consuming optimization when dealing with new identification tasks. An associative memory is designed to realize dimension reduction, knowledge learning and transfer between different identification tasks. Agents can exploit the optimal knowledge from source tasks to accelerate the search rate in new tasks and improve solution accuracy. A greedy action selection rule is adopted for agents to balance the global and local search. The performance of the proposed ITQ approach has been validated on a 68-bus test system. Simulation results in multi-test cases verify that the proposed method is robust and can estimate load parameters accurately. Comparisons with other methods show that the proposed method has superior convergence rate and stability.

Index Terms—Load modeling, parameter identification, transfer learning, reinforcement learning, imitation learning.

I. INTRODUCTION

AS AN important part of power system analysis, electrical load modeling has a critical impact on the stable operation of power grids [1]–[3]. Incorrect load models may lead to completely biased results for system operation status and stability evaluation [4]–[7]. Due to time-variability, complex composition and non-linearity, fast and accurate load modeling still remains a challenging problem. Therefore, it is imperative to identify load model parameters accurately and rapidly to help provide more reliable results for real-time power system operation.

Manuscript received November 18, 2019; revised May 11, 2020 and July 20, 2020; accepted September 17, 2020. This work was supported by the Power Systems Engineering Research Center under Grant PSERC S-84G. Paper no. TSG-01746-2019. (*Corresponding author: Zhaoyu Wang.*)

Jian Xie, Zixiao Ma, Kaveh Dehghanpour, and Zhaoyu Wang are with the Department of Electrical and Computer Engineering, Iowa State University, Ames, IA 50011 USA (e-mail: jianx@iastate.edu; zma@iastate.edu; kavehd@iastate.edu; wzy@iastate.edu).

Yishen Wang, Ruisheng Diao, and Di Shi are with the Department of AI and System Analytics, GEIRI North America, San Jose, CA 95134 USA (e-mail: yishen.wang@geirina.net; ruisheng.diao@geirina.net; di.shi@geirina.net).

Color versions of one or more of the figures in this article are available online at <http://ieeexplore.ieee.org>.

Digital Object Identifier 10.1109/TSG.2020.3025509

AQ2

Based on load models' characteristics, conventional load models can be categorized into three types: static load models, dynamic load models and composite load models. In static load models, active and reactive power can be expressed as functions of bus voltage and frequency. Common static load models include static load model which comprised of constant impedance Z , constant current I and constant power P loads (ZIP) model [8] and exponential model [9]. Dynamic load models can represent the relationship between load active/reactive power and bus voltage. Representative dynamic loads are induction motor (IM) load and exponential recovery load model (ERL) [10]. IM load model is considered to be a physical model since it is derived from the equivalent circuit of an IM [11]. Numerous studies have shown that a single static or dynamic model cannot sufficiently replicate the dynamic behavior of the actual load. Therefore, composite load models, combining ZIP and IM have been adopted by most of the utilities to represent the actual load, which can provide more accurate characteristics [12].

Previous works have focused on measurement-based load identification and parameter estimation. Measurement-based methods can be classified into two categories: artificial neural network (ANN)-based methods and optimization-based methods. The ANN-based methods do not require any pre-defined physical load models and can update load outputs (i.e., active and reactive powers of loads) using the measurements in real-time. A deep learning-based technique was proposed in [13] to identify time-varying load parameters.

Optimization-based parameter estimation algorithms usually pre-define a load structure and then try to search for the optimal parameters to minimize the error between the actual power measurements and the estimated power responses. These methods can be divided into statistical techniques and heuristic techniques. Common statistical search techniques include least square (LS) method, maximum likelihood method and gradient-based method. In [14], a weighted LS method was utilized to estimate the parameters of a first order IM. However, LS methods are sensitive to outliers. Also, it can be difficult to determine the exact load parameters when the estimation process is performed over only a small number of replicated observations. A maximum likelihood approach was adopted in [15] to estimate load parameters. The two disadvantages of this method are that it is based on strong assumptions on the data structure and is sensitive to the choice of initial values. In [16], a gradient-based method was proposed to estimate

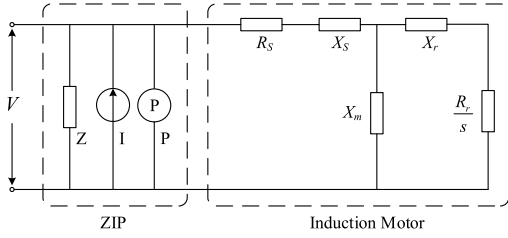


Fig. 1. Equivalent circuit of composite ZIP and IM load model [3].

parameters of a fifth-order IM load. However, gradient-based methods are sensitive to the learning rate and depend on proper initialization.

As for heuristic techniques, genetic algorithm (GA) [2] has been widely adopted to estimate the parameters of load models. GA-based methods are sensitive to the distribution of initial population of candidate solvers. In addition, premature convergence is another issue that should be considered when solutions are generated. An improved particle swarm optimization (IPSO) method has been applied in [17] to identify the unknown composite load model parameters. Unfortunately, most of the above methods are unable to exploit the prior optimization knowledge when dealing with new optimization tasks, which will result in an inefficient search when dealing with new load parameter identification tasks.

In this article, we cast the optimization problem of parameter identification for composite load model as a learning task. In applications involving non-linear optimization problems, reinforcement learning (RL) methods have been adopted to efficiently obtain optimal solutions [18]. During the RL process, agents execute actions and update their states based on designed exploration and exploitation rules. When applying RL method in power system, agents can be viewed as the candidate solutions, such as estimated load parameters; actions are used to tune the position of agents, i.e., tune the value of estimated load parameters. As an efficient RL method, Q-learning has been widely used for online optimization and control [19], [20]. However, similar to heuristic approaches, RL methods can suffer from inability to store prior agent knowledge since the initial state and action values are usually set to zero when dealing with a new optimization task, which results in time-consuming performance when identifying a large number of load parameters.

Recently, *transfer learning* has emerged as a more suitable alternative due to its ability to compensate the shortcoming of conventional RL by exploiting the prior knowledge obtained in previous time periods (i.e., source optimization tasks) [21]. This can significantly reduce the computational time for load parameter identification. In addition, imitation learning can guide a RL agent to take a more effective exploration at the initial period of RL search process and improve the exploration efficiency. Motivated by the advantages of imitation learning, a novel Imitation and Transfer Learning based Q-learning (ITQ) approach is proposed in this article, which aggregates Q-learning, transfer learning and imitation learning. The proposed method mitigates the computational burden and improves the accuracy of load parameter identification.

The main contributions of this article can be summarized as follows:

- In the pre-learning stage of dealing with source optimization tasks, imitation learning is introduced to guide the RL agent to execute a more informative exploration instead of a random one.
- When dealing with a new identification task, knowledge transfer process is conducted based on the similarity between new tasks and source tasks to help a RL agent to effectively perform generalizations based on its previous experiences that are encoded within a pre-learned knowledge matrix.
- A swarm of agents are employed in the learning process to further accelerate learning rate. These interactive agents update their knowledge matrices simultaneously and share their optimal solutions during learning process.
- A greedy random search rule is developed in RL process to ensure that the proposed method can obtain high quality solutions over time.

The rest of this article is structured as follows: Section II describes the composite load model structure. Section III presents the basic principles of ITQ. The framework of ITQ based load model parameters identification is given in Section IV. Simulation results are presented in Section V, and Section VI concludes this article.

II. COMPOSITE LOAD MODEL STRUCTURE

An equivalent circuit of composite load model, consists of static ZIP and dynamic IM components connected in parallel is shown in Fig. 1. The mathematical descriptions of the active and reactive power of the ZIP component are expressed as follows:

$$P_{ZIP} = P_{ZIP,0} \left(a_p \left(\frac{V}{V_0} \right)^2 + b_p \left(\frac{V}{V_0} \right) + c_p \right) \quad (1)$$

$$Q_{ZIP} = Q_{ZIP,0} \left(a_q \left(\frac{V}{V_0} \right)^2 + b_q \left(\frac{V}{V_0} \right) + c_q \right) \quad (2)$$

where $P_{ZIP,0}$, $Q_{ZIP,0}$, V_0 are active, reactive power and root-mean-square (RMS) value of voltage in the steady state before disturbance and V is the bus voltage magnitude at a given time. In addition, ZIP parameters a_p , b_p and c_p satisfy $a_p + b_p + c_p = 1$, and a_q , b_q and c_q satisfy $a_q + b_q + c_q = 1$.

The parameters of the IM component include: stator resistance R_s , rotor resistance R_r , stator reactance X_s , and rotor reactance X_r , magnetizing reactance X_m , and the slip s .

The IM component dynamics can be expressed as follows:

$$\frac{dE'_d}{dt} = -\frac{R_r}{X_r + X_m} \left(E'_d + \frac{X_m^2}{X_r + X_m} I_q \right) - (\omega - 1) E'_q \quad (3)$$

$$\frac{dE'_q}{dt} = -\frac{R_r}{X_r + X_m} \left(E'_q - \frac{X_m^2}{X_r + X_m} I_d \right) + (\omega - 1) E'_d \quad (4)$$

$$\frac{d\omega}{dt} = -\frac{1}{2H} \left[T_0 (A\omega^2 + B\omega + C) - (E'_d I_d + E'_q I_q) \right] \quad (5)$$

where H is the rotor inertia constant; A , B and C denote the torque coefficients and satisfy $A\omega^2 + B\omega + C = 1$; $\omega = 1 - s$ represents the rotation speed of the induction motor; E'_d and E'_q

175 refer to the d -axis and q -axis transient electromagnetic fields
 176 (EMF) of the IM. I_d and I_q are the d and q axes currents, with
 177 detailed expressions given in [3].

178 Given the dynamic states, parameters and bus voltage, the
 179 active and reactive power of the IM model are determined as
 180 follows:

$$181 \quad P_{IM} = U_d I_d + U_q I_q \quad (6)$$

$$182 \quad Q_{IM} = U_q I_d - U_d I_q \quad (7)$$

183 where the d -axis bus voltage U_d and the q -axis bus voltage
 184 U_q satisfy the following equation:

$$185 \quad V = \sqrt{U_d^2 + U_q^2} \quad (8)$$

186 By aggregating the ZIP and IM active (reactive) powers, we
 187 can obtain the total active and reactive power of the composite
 188 load model [3]. In addition, another important parameter of the
 189 composite load model, is the ratio of the initial active power
 190 of the IM to the total load, which is defined as:

$$191 \quad K_{pm} = \frac{P_{Im,0}}{P_0} \quad (9)$$

192 where P_0 denotes the initial active power of the composite
 193 load before disturbance and $P_{Im,0}$ is the initial active power
 194 of the equivalent IM.

195 Traditionally, the 13 parameters in equations (1)-(9) which
 196 have to be identified to fully capture the composite model, are
 197 as follows:

$$198 \quad \theta = [R_s, X_s, X_m, X_r, R_r, H, A, B, a_p, b_p, a_q, b_q, K_{pm}]$$

199 The parameter identification process can be written as an
 200 optimization problem with the objective function of min-
 201 imizing the sum of squared difference between the esti-
 202 mated active/reactive power and the measured active/reactive
 203 power, as:

$$204 \quad \min_{\theta} h(\theta) = \frac{\sum_{k=1}^L [(P_{\theta}(k) - P(k))^2 + (Q_{\theta}(k) - Q(k))^2]}{L} \quad (10)$$

205 where L is the number of measurement samples; $P_{\theta}(k)$ and
 206 $P(k)$ are the estimated and measured active power; $Q_{\theta}(k)$ and
 207 $Q(k)$ are estimated and measured reactive power; h is the
 208 objective function representing the load model output error.

209 III. BASIC PRINCIPLES OF ITQ

210 The overall process of implementing the ITQ is shown
 211 in Fig. 2, which includes 4 main steps: 1) RL agents learn
 212 the optimal solution for source identification tasks based on
 213 Q-learning method and store the optimal knowledge (solu-
 214 tion) in knowledge matrix (Q-table); 2) Other agents adopt
 215 Levenberg-Marquardt algorithm (L-M) [2] to deal with the
 216 source tasks and RL agents learn from them for a more effi-
 217 cient search during the initial phase via imitation learning;
 218 3) When dealing with a new load parameter identification task,
 219 defining and computing the similarities between source tasks
 220 and new task; 4) estimating the optimal knowledge matrix for
 221 the new task by exploiting the previous optimal knowledge
 222 via transfer learning.

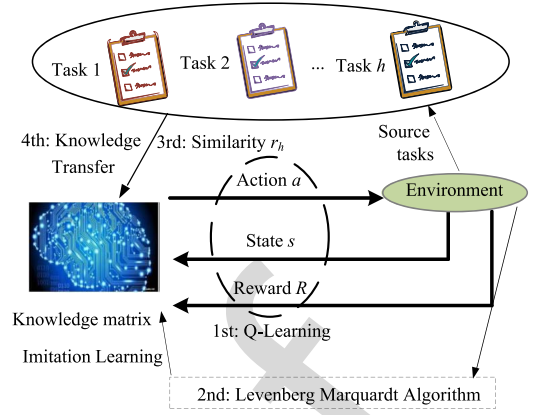


Fig. 2. Basic principle of ITQ method.

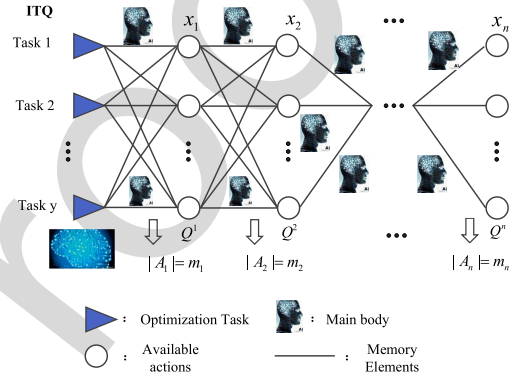


Fig. 3. Basic principle of associate memory.

223 A. Q-Learning

224 Similar to other classical RL methods, Q-learning aims to
 225 obtain an optimal policy such that a reward, R , is maximized.
 226 In the Q-learning algorithm, an agent observes the current state
 227 s and executes an action a . The system observes the corre-
 228 sponding results and samples a reward to the agent. The agent
 229 receives the reward and updates the Q-value corresponding
 230 to the action-state, which represents the expected estimated
 231 accumulated reward for the action-state pair. After each state
 232 transition, a new action is selected, resulting in a new state
 233 and a new reward. By continuous exploitation and explora-
 234 tion, the agent will eventually obtain the optimal Q-table
 235 which determines the action selection policy. In load param-
 236 eter identification task, each agent can be viewed as a particle
 237 which contains estimated load parameters; actions are used
 238 to tune the value of estimated load parameter. However, there
 239 are two disadvantages for traditional Q-learning method: 1) the
 240 dimension of Q-table will increase dramatically if the number
 241 of controllable variables or the alternative actions increase;
 242 2) using a single RL agent leads to a low knowledge learning
 243 efficiency.

244 However, the curse of dimensionality will emerge if the
 245 number of controllable variables grows too large in conven-
 246 tional Q-learning. Assuming that the number of alternative
 247 actions for a controllable variable x_i to be m_i , then the dimen-
 248 sion of action set $|\mathbf{A}| = m_1 m_2 \cdots m_n$, where n is the number
 249 of controllable variables. If n increases significantly, the space

and time complexity will increase hugely and the problem becomes intractable.

In order to avoid the curse of dimensionality, an associative memory is adopted to reduce the state-action space by decomposing the large-scale knowledge matrix (Q-table) into multiple lower-dimensional spaces [19]. As illustrated in Fig. 3, instead of adopting an extremely large-scale action set $|\mathbf{A}|$ to denote the optimization space of all the controllable variables, the multiple small-scale action sets $(\mathbf{A}_1, \mathbf{A}_2, \dots, \mathbf{A}_n)$ are adopted to represent the action space of each controllable variable. Consequently, each controllable variable has a corresponding memory matrix Q_i . Under such framework, the dimension of memory matrix can be greatly decreased.

Hence, each variable has a corresponding knowledge matrix. Once the action of the previous variable is determined, this action is taken as the state of the next variable, thereby forming a chain connection. By adopting the associative memory, the physical meaning of state is the same as action for load parameter identification task. A swarm of agents are adopted to improve the knowledge learning rate as there are multiple agents executing actions at the same time, which leads to simultaneous updates in Q-values of multiple state-action pairs. After introducing the swarm of agents, the i th memory matrix can be updated as:

$$\begin{cases} Q_{k+1}^i(s_k^{ij}, a_k^{ij}) = Q_{k+1}^i(s_k^{ij}, a_k^{ij}) + \alpha \Delta Q_k^i \\ \Delta Q_k^i = R^{ij}(s_{k+1}^{ij}, s_k^{ij}, a_k^{ij}) + \gamma \max_{a^i \in A_i} Q_k^i(s_k^{ij}, a_k^{ij}) \\ \quad - Q_k^i(s_k^{ij}, a_k^{ij}) \end{cases} \quad (11)$$

where α is the learning rate; i ($i = 1, 2, \dots, n$) denotes the i th variable and j ($j = 1, 2, \dots, L$) represents the j th agent; n and L are the number of variables and agents, respectively; γ is the discount factor; subscript k denotes the iteration number; A_i denotes to the action space of agent i . ΔQ is the knowledge increment; (s_k, a_k) denotes the state-action pair at the k th iteration; $R(s_{k+1}, s_k, a_k)$ is the feedback reward of transition from state s_k to s_{k+1} after executing action a_k .

RL methods often adopt a pure strategy of greedy actions or a random global search strategy. In general, local search based on greedy strategy tends to cause the algorithm to fall into a local optimum, while random global search strategy tends to result in a long optimization time. Therefore, this article uses the ε -greedy strategy [18] to effectively balance the local search and the global search, as follows:

$$a_{k+1}^{ij} = \begin{cases} \arg \max_{a^i \in A_i} Q_k^i(s_{k+1}^{ij}, a^i), & \text{if } \varepsilon \leq \varepsilon_0 \\ a_s & \text{Otherwise} \end{cases} \quad (12)$$

where ε_0 is a random number with a probability uniformly distributed in $[0, 1]$; ε is the exploitation rate representing the probability of a greedy action (exploitation); a_s denotes a random action (global search).

After agents execute their actions, a reward is received to evaluate corresponding state-action pair by each agent. In general, an agent will receive a larger reward if the executed action results in a better solution (i.e., smaller objective value).

Hence, the reward rule is designed as follows:

$$R^{ij}(s_{k+1}^{ij}, s_k^{ij}, a_k^{ij}) = \begin{cases} \frac{1}{h_j^{k+1}}, & \text{if } h_j^{k+1} \leq h_j^k \\ 0, & \text{otherwise} \end{cases} \quad (13)$$

where h_j^k is the objective function of the j th agent after the k th iteration.

B. Learning Efficiency Improvement via Imitation Learning

For a new identification task, RL agents need to execute a series of random exploitation and exploration processes to obtain the optimal policy, which consumes quite a long time without any prior knowledge and cannot meet the requirement for online load identification.

Thus, imitation learning is adopted in this section to accelerate the random search process during the initial phase of search. In the imitation process, RL agents can be regarded as *students*, which can learn and imitate other *teachers* with more knowledge. In order to better guide the RL agents to update the knowledge matrix during the initial phase, a highly efficient L-M method is adopted as the teacher. The L-M algorithm is a gradient descent method. The parameter set θ updating process for L-M method is as follows:

$$\theta_{i+1} = \theta_i + (J^T J + \lambda I)^{-1} J^T h(\theta_i) \quad (14)$$

where θ_i denotes the estimated parameter set in the i th iteration step; J is the Jacobian matrix which can be obtained by calculating the first-order partial derivatives of estimated outputs to each parameter; λ represents the step size and I is the identity matrix.

In addition, L-M is sensitive to initial conditions and may diverge outside of the defined ranges or be trapped in a local optimal solution. In order to address these issues, some agents learn knowledge from L-M to select the state-action pair and update the knowledge matrix, the other agents update knowledge based on Q-learning and ε -greedy rule shown in (12). After each iteration, the rewards of all agents are calculated, shared and sorted. The corresponding state-action pair with the largest reward is transmitted to all imitative teachers (L-M agents). In a new iteration, the agents with larger rewards execute actions based on Q-learning principle with ε -greedy policy, while other agents with smaller reward learn from L-M to select state-action pair.

C. Knowledge Transfer via Transfer Learning

Transfer learning can be applied to discover domain-invariant intrinsic features and structures underlying two different but related domains, which establishes successful transfer and re-utilization of data information across domains. ITQ agents obtain optimal knowledge matrices (Q-tables) for source parameter identification tasks (source tasks) during the pre-learning process, the prior knowledge are then exploited as the initial knowledge matrices of a new parameter identification task (new task), thereby avoiding agents' blind explorations and improving search efficiency. This transfer

TABLE I
NUMERICAL INTERVAL OF LOAD PARAMETERS

Parameter	R_s	X_s	X_m	R_r	X_r
Range	[0.02,0.2]	[0.1,0.2]	[2,3.8]	[0.01,0.1]	[0.07,0.18]
Parameter	K_{pm}	H	A	B	a_p
Range	[0.2,0.9]	[0.5,2]	[0.2,1]	[0,1]	[0.1,0.9]
Parameter	b_p	a_q	b_q		
Range	[0.1,0.9]	[0.1,0.9]	[0.1,0.9]		

process is designed as:

$$Q_{ni}^0 = \sum_{e=1}^E r_e Q_{ei}^*, \quad i = 1, 2, \dots, N \quad (15)$$

where Q_{ni}^0 denotes the initial knowledge matrix of the i th variable in the new task; Q_{ei}^* represents the optimal knowledge matrix of the i th parameter in the e th source task; r_e represents the similarity between the new task and the e th source task and the detailed definition of similarity between two load parameter identification tasks are described in Section IV; E denotes the number of the source task.

IV. DESIGN OF ITQ FOR LOAD PARAMETER IDENTIFICATION

In this section, the detailed steps and overall procedure to apply ITQ for load parameter identification are introduced according to the principle of ITQ.

A. Action-State Design

Although load parameters of the power system vary at different times, they always change around typical values. A larger range will affect the speed and accuracy of the algorithm, while a smaller range may exclude actual values. Therefore, in addition to algorithm performance, the range of each load parameter should be pre-designed based on its typical value in real power systems. In this article, the range of the parameter to be identified is proposed based on the typical value in actual power systems and the former related research in [12], [17], [22], as shown in Table I.

In general, the standard Q-learning algorithm is based on discrete Markov processes, which cannot be directly applied to the solution of continuous variables optimization problems. The discretization method is the most direct means to solve this problem at present. Hence, the continuous variables are divided into discrete intervals to approximate the optimal solution of the original problem with sufficient accuracy. In this article, the searching space of each continuous parameter is divided into 50 parts. For example, the search space for m_i which denotes the i th parameter in θ is $[m_{i1} \ m_{i2} \ \dots \ m_{i50}]$, which is sorted in an increasing order. To associate ITQ method with load parameters identification, we can define $Id_i \in [1, 50]$ as an index for the i th load parameter. Then, state s_i can be viewed as the current index of the i th estimated load parameter, that is $s_i = Id_i$. For

instance, $s_i = 3$ means current estimation of the i th parameter is the 3rd number within the 50 parts.

Then, the action of each variable (load model parameter) is defined by:

$$\mathbf{A}_i = \{a_{i,1} \ a_{i,2} \ \dots \ a_{i,50}\} \quad (16)$$

where \mathbf{A}_i denotes the i th variable's action set; $a_{i,k}$ ($k = 1, 2, \dots, 50$) denotes the k th action of the i th load parameter. For instance, $a_i = 5$ means the agent selects the 5th number within the 50 parts for current iteration episode. As stated in Section III, the action set of each variable is the state set of the next variable, i.e., $\mathbf{A}_i = \mathbf{S}_{i+1}$. For the first variable, the state set is equivalent to the action set.

B. Reward Function Design

According to the description in Section III, the reward of each agent can be obtained by (13) after each iteration and a smaller objective lead to a larger reward.

C. Knowledge Transfer Design

The key to determine the transfer quality is the definition of the similarity between source task and new task. From (10) we can see that the optimization task of load parameters identification is determined by the bus voltage, active and reactive power. Hence, Fréchet distance [23] is adopted to measure the similarity between bus voltage curves, active and reactive power curves in the source tasks and new task. The Fréchet distance between the two curves is the length of the shortest leash sufficient for both to traverse their separate paths, which takes into account the location and ordering of the points along the curves. This method is widely used in curve similarity analysis. Let \mathbf{F} and \mathbf{G} be the bus voltage curves in the source task and new task, and the length for each curve are \mathbf{T} and \mathbf{W} . The bus voltage in the source task is given as a function of time by $\mathbf{F}(\alpha(t))$ and $\mathbf{G}(\beta(t))$, where $\alpha(t)$ and $\beta(t)$ are two increasing functions and $\alpha(0) = 0$, $\alpha(1) = \mathbf{T}$, $\beta(0) = 0$, $\beta(1) = \mathbf{W}$. Mathematically, the Fréchet distance between the two curves is defined as:

$$\delta_F(F, G) = \inf_{\alpha, \beta} \max_{t \in [0,1]} \{d(F(\alpha(t)), G(\beta(t)))\} \quad (17)$$

where d is the Euclidean distance function.

Hence, the similarity between two bus voltage curves is determined by the equation:

$$SU(F, G) = 1 - \frac{\inf_{\alpha, \beta} \max_{t \in [0,1]} \{d(F(\alpha(t)), G(\beta(t)))\}}{\sup_{\alpha, \beta} \max_{t \in [0,1]} \{d(F(\alpha(t)), G(\beta(t)))\}} \quad (18)$$

where $SU(F, G) \in [0, 1]$, a value near 1 indicates more similarity between the two curves, while a value near 0 indicates less similarity between them.

Similarly, Fréchet distance between active (reactive) power curves are noted as SP and SQ . Then, similarity between the source load parameter identification tasks and the new identification task is defined as:

$$r = 1/3(SU + SP + SQ). \quad (19)$$

436 D. ITQ Parameters Setting

437 Suitable parameters can improve the performance of ITQ
438 and reduce the calculation time, hence, it is crucial to choose
439 appropriate parameters based on the generic guidelines [18]:

- 440 • The learning rate α directly determines to what extent
441 newly acquired information overrides old information.
442 A larger α can achieve a faster convergence rate but
443 with a higher probability of falling into the local optimal
444 solution. Conversely, a smaller α can lead to a slower
445 convergence rate but ensure a higher-quality solution.
- 446 • The discount factor γ determines the importance of
447 future rewards. Since the current optimal solution of load
448 parameters is significant, a smaller γ should be chosen.
- 449 • The exploration rate ϵ allows agents to explore new action
450 with a certain probability. A larger ϵ drives agents to
451 select a greedy action rather than explore a random action.

452 Based on the guidelines, the four parameters of ITQ for
453 load parameter identification can be chosen by a few trial-and
454 error experiments and are shown in Table II. Case studies in
455 Section V verify that these values can be viewed as a general
456 parameters for load parameter identification task.

457 E. Overall Procedure

458 The overall process to implement the approach is shown
459 in Fig. 4, where k_{max} denotes the maximum iteration steps
460 and $\|Q_i^{k+1} - Q_i^k\|_2$ is the Euclidean norm of Q -value differ-
461 ences, and ζ is the convergence coefficient. As shown in Fig. 4,
462 the pre-learning process is firstly executed to accumulate the
463 optimal knowledge from the source tasks, then, agents' action
464 strategy in the new task is initialized with transfer learning,
465 thereby accelerating the optimization process. In real power
466 systems, dynamic measurements can be collected after distur-
467 bance which happens in chronological order. The source
468 task is to identify load parameters after an earlier disturbance,
469 while the new task is the identification task based on later
470 disturbance.

471 V. CASE STUDY

472 This section evaluates the effectiveness of the proposed
473 approach. The estimated results from ITQ are compared with
474 that of the whale optimization algorithm (WOA) [24], Grey
475 wolf optimizer (GWO) [24], IPSO [17], and classical L-M
476 method [2]. These methods are newly invented and has been
477 verified that they outperform GA and PSO. In order to gener-
478 ate the fault data, dynamic simulations are conducted on the
479 New England 68-bus test system with composite ZIP and IM
480 loads [13]. All simulations are undertaken in MATLAB Power
481 System Tool (PST) and the sampling rate is 100Hz. The popu-
482 lation size and the maximum iteration step are set as 30 and
483 1000 for each heuristic optimization algorithm. For ITQ, the
484 parameters are shown in Table II.

485 A. Simulation Model

486 The 68-bus test system is a reduced-order model of the New
487 England/New York interconnected system [13]. It contains 16
488 generators, 68 buses and 29 loads. Each load is described
489 as a composite load with ZIP and IM. Load parameters

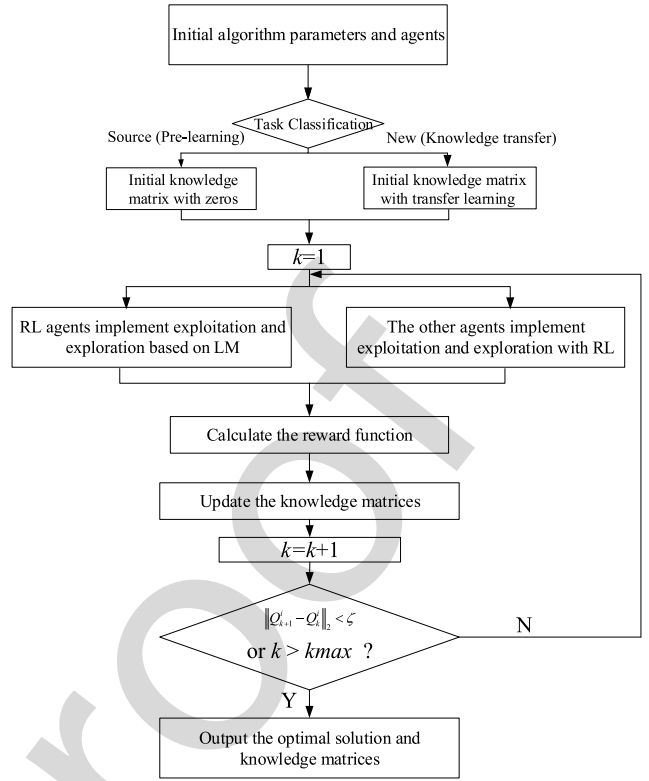


Fig. 4. Overall Procedure of ITQ.

TABLE II
PARAMETERS USED IN ITQ

Parameter	Pre-learning	Transfer learning
α	0.1	0.1
γ	0.2	0.1
ϵ	0.5	0.8

identification process is carried out for the load connected to bus 27.

B. Pre-Learning Process

492 A pre-learning process needs to be firstly executed to accu-
493 mulate the optimal knowledge matrices from the source tasks
494 for ITQ algorithm. Therefore, 5 different tasks are simulated
495 and tasks 1 and 2 are taken as source tasks. True load param-
496 eters in each task are shown in Table III. In task 1 and 3, fault
497 occurs on the line between bus 60 and bus 61; in task 2 and 4,
498 fault occurs on the line between bus 18 and bus 49; in task 5,
499 fault occurs on the line between bus 19 and bus 68. The Fault
500 type is three phase fault in all tasks.
501

502 As stated in Section III, an associative memory is designed
503 to realize dimension reduction by decomposing the large-scale
504 knowledge matrix (Q-table) into multiple lower-dimensional
505 spaces. For all case studies in this article, since the search-
506 ing space of each continuous parameter is divided into 50
507 parts, the dimensions of each low dimensional Q table is set
508 to be 50×50 .

509 In the pre-learning process, RL agents are initialized as
510 zeros and a random initialization is adopted to determine the

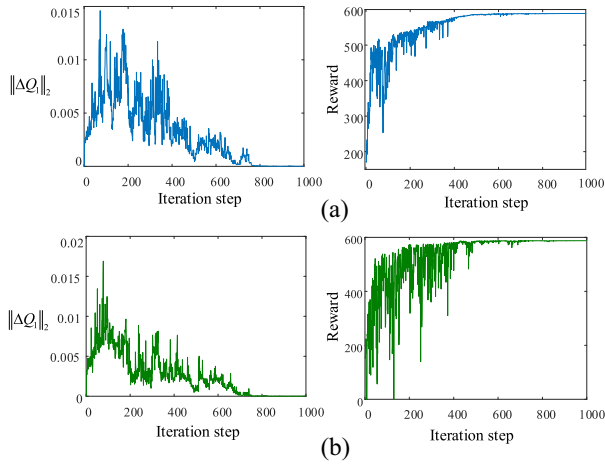


Fig. 5. Convergence of the memory matrices and reward obtained by an agent in two tasks.

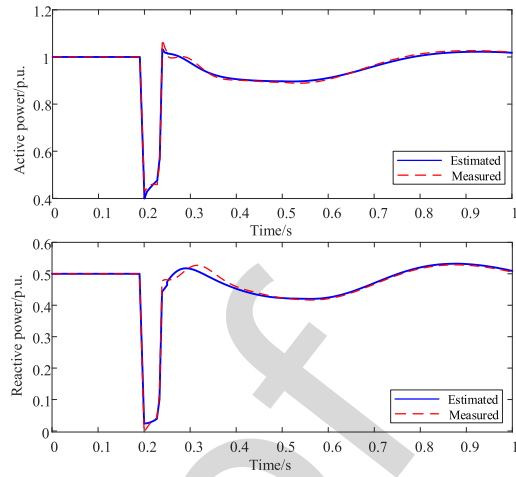


Fig. 7. Comparison between measurements and estimated outputs.

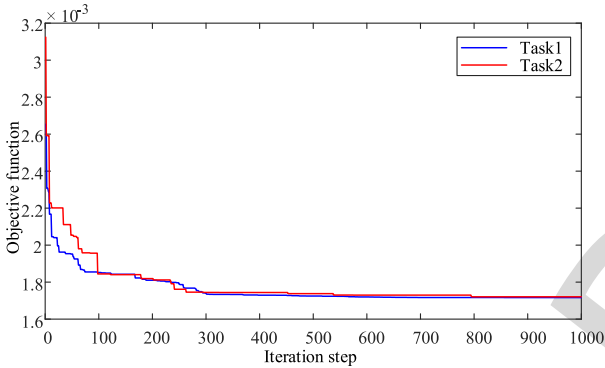


Fig. 6. Convergence of the objective functions.

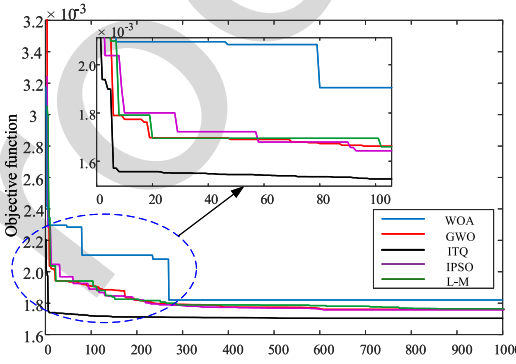


Fig. 8. Objective function obtained by five methods.

511 initial set of L-M agents. Fig. 5 shows the convergence curve
 512 and the reward obtained by an agent during the pre-learning
 513 process in two tasks. It is clear that each variable can converge
 514 to its own optimal knowledge matrix after 700 iteration steps.
 515 The optimal objective function during the learning process
 516 among all agents is shown in Fig. 6. It is clear that ITQ can
 517 converge to the optimal knowledge matrices for source task 1.
 518 Similarly, when applying the pre-learning process to task 2,
 519 a high quality fitness function can be obtained, as shown in
 520 Fig. 6. Fig. 7 presents the comparison between the estimated
 521 power outputs and measurements. It can be seen that the esti-
 522 mated outputs are very close to measurements. These results
 523 validate the highly convergence of the proposed ITQ method.

524 *C. Transfer Learning and Comparison*

525 With the pre-learning process completed, the optimal knowl-
 526 edge matrices are exploited for the online load parameters
 527 identification tasks using transfer learning. The online identi-
 528 fication is implemented for task 3. As ITQ agents has learned
 529 the optimal knowledge from task 1 and task 2, these tasks can
 530 be viewed as source when dealing with task 3. Then, based on
 531 the definition of similarity in (19), we can compute similar-
 532 ities $r_{13} = 0.63$ and $r_{23} = 0.71$. Therefore, knowledge matrix
 533 for task 3 can be initialized based on (19).

534 Fig. 8 compares the convergence of the objective function
 535 for task 3 obtained by ITQ and other 4 algorithms, including

WOA, GWQ, IPSO and L-M. Reward for these optimization 536
 methods are defined as $1/h$ and h denotes the objective func- 537
 tion. Note that all the algorithms adopt a random initializa- 538
 tion except the proposed ITQ which is able to transfer opti- 539
 mal knowledge from source tasks. From Fig. 8, it is clear that 540
 ITQ can perform deep exploitation from source tasks when 541
 dealing with a new task and it can obtain the optimal solu- 542
 tion within 150 iteration steps, which is much faster than that 543
 of the pre-learning process. The comparison verifies that the 544
 convergence rate can be dramatically accelerated by transfer 545
 learning. Compared with other methods, ITQ converge the 546
 faster and can obtain a better reward. In addition, ITQ can 547
 obtain a higher quality reward contributed to the fact that 548
 random search agents can avoid the premature convergence 549
 and search the globe optimal result. In order to further test 550
 the performance of ITQ, all the algorithms are executed with 551
 100 runs. Fig. 9 shows the Box plots of objective functions 552
 obtained by the 5 algorithms, and it is clear that ITQ per- 553
 forms best and the convergence stability is higher than other 554
 algorithms. 555

556 *D. Impact of Low Similarity and Limited Source Tasks*

557 This section validates the effectiveness of ITQ with low sim- 558
 ilarity and limited source tasks. In real power systems, limited 559
 source tasks can be an obstacle for transfer learning. 560

TABLE III
PRE-SET PARAMETERS FOR DIFFERENT TASKS

Task	R_s	X_s	X_m	X_r	K_{pm}	R_r	a_p	a_q	b_p	b_q	H	A	B
1	0.045	0.173	2.49	0.131	0.43	0.031	0.40	0.30	0.30	0.30	1.2	0.9	0.10
2	0.113	0.104	2.21	0.081	0.71	0.045	0.55	0.25	0.15	0.35	1.1	0.5	0.83
3	0.188	0.145	3.35	0.151	0.55	0.065	0.30	0.20	0.40	0.40	0.7	0.9	0.51
4	0.151	0.112	2.83	0.163	0.62	0.021	0.61	0.15	0.23	0.42	1.4	0.7	0.29
5	0.072	0.152	3.22	0.097	0.33	0.071	0.33	0.27	0.57	0.31	0.9	0.3	0.90

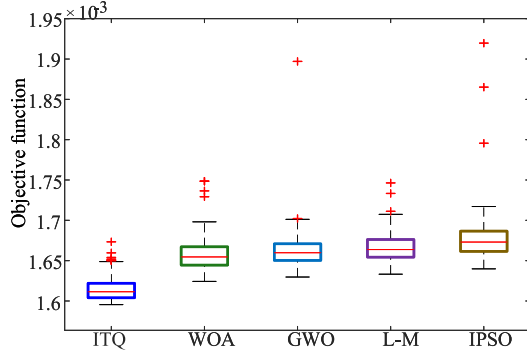


Fig. 9. Comparison of Box plot of objective function.

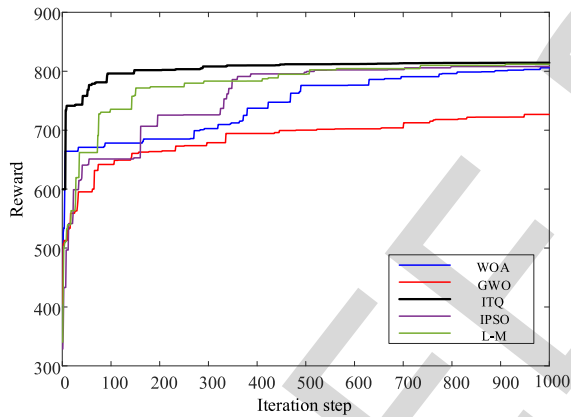


Fig. 10. Reward comparison under low similarity condition.

Similarity analysis shows that $r_{14} = 0.51$ and $r_{24} = 0.33$, and this indicates that there are few similarities between task 4 and another 2 source tasks. ITQ are adopted for task 4 to test the performance of ITQ when dealing with a new task with low similarity. Fig. 10 shows the comparison of optimization results obtained by 5 methods. It indicates that each algorithm can obtain a satisfied results and ITQ presents the biggest reward which means ITQ still has high performance even when the similarity between new task and source task is low.

Table IV presents identified results (average) from different algorithms for load parameters in task 4. For each algorithm, 150 trials have been run to obtain the optimal load parameters. For other methods, the initial set of parameters in the first trial are randomly generated and will be used for initialization in the remaining 149 trials. For ITQ, the initial knowledge matrices are the same and calculated by (15) and 19 in each trial. From the comparison results, it is clear that ITQ-based

TABLE IV
COMPARISON OF ESTIMATED PARAMETERS

Parameter	Method					
	True	ITQ	WOA	GWO	IPSO	L-M
R_s	0.151	0.1583	0.1622	0.1631	0.1628	0.1621
X_s	0.112	0.1255	0.1285	0.1311	0.1325	0.1293
X_m	2.83	2.909	3.11	3.023	3.152	3.106
X_r	0.163	0.1711	0.1832	0.1921	0.1865	0.1955
K_{pm}	0.62	0.6531	0.5885	0.6959	0.6941	0.5773
R_r	0.021	0.0358	0.0322	0.0395	0.0388	0.0331
a_p	0.61	0.5606	0.6963	0.5112	0.5232	0.6885
a_q	0.15	0.1889	0.2213	0.2515	0.2332	0.2106
b_p	0.23	0.2939	0.3121	0.2882	0.3351	0.3025
b_q	0.42	0.3101	0.2859	0.1865	0.2688	0.3232
H	1.4	1.611	1.052	1.857	1.212	1.0886
A	0.7	0.7414	0.7818	0.6543	0.6852	0.7665
B	0.29	0.3232	0.2516	0.3568	0.2158	0.3312

load parameters are closest to actual values and this is consistent with the results in Fig. 8. There are small discrepancies between estimated parameters and true values, which may be caused by the limited observability of some parameters.

E. Robustness of ITQ

Due to the complexity and nonlinearity of load models, it has been found that different load parameter combinations may lead to the same or similar dynamic response. For example, given a set of measured data (U , P and Q), multiple combinations of load model parameters may result in a same or similar reward using previous optimization methods. To test the robustness of the proposed method in searching the optimal parameters, 150 trials have been carried out for task 4 and the final reward and optimal parameters are recorded. The reward under each trial is shown in Fig. 11 and it is clear that the optimal rewards do not change much. But for other heuristic methods, rewards have large variances in 150 trials. Based on the study in [7], the eight parameters R_s , R_r , X_r , K_{pm} , a_p , b_p , a_q , b_q have the highest impact on load dynamics and can be identified, while other five parameters X_s , X_m , H , A , B do not affect load dynamics and cannot be identified from voltage disturbance. Therefore, we focus on the identification results of these eight parameters.

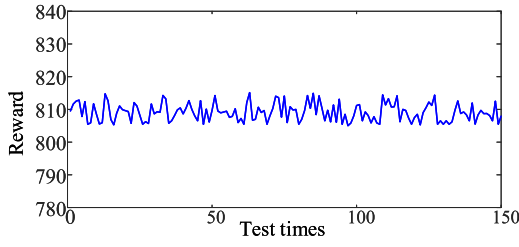


Fig. 11. Optimal reward under 150 optimization trials.

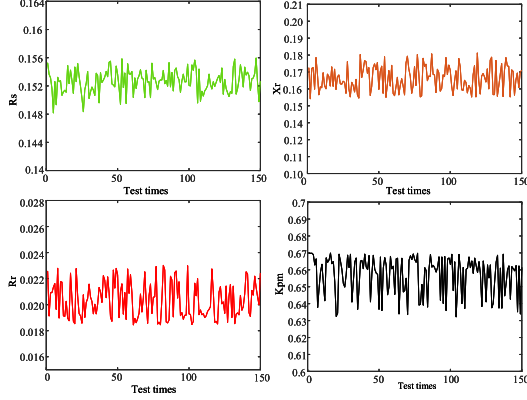


Fig. 12. Identified parameters of IM under 150 optimization trials.

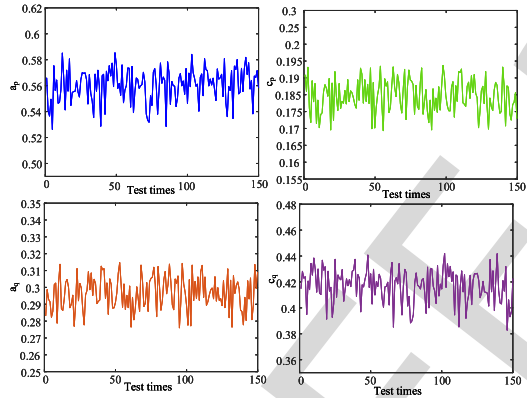


Fig. 13. Identified parameters of ZIP under 150 optimization trials.

600 Fig. 12 and Fig. 13 present the optimal results of these eight
 601 parameters under 150 trials. The parameters shown in these
 602 two figures are the optimal results (actions) obtained from
 603 each optimization process. It can be seen that the results of
 604 these eight parameters do not have large variances and are con-
 605 sistent with the corresponding true values, which corroborate
 606 the robustness of the proposed method.

607 In addition, as shown in Fig. 5, for a certain optimization
 608 process, the reward of the proposed ITQ method converges
 609 rapidly. In order to verify that identified parameters converge
 610 with the same rate during the RL process, Fig. 14 shows the
 611 curve of four parameters R_s , R_r , X_r , K_{pm} at each iteration step.
 612 The result is based on the data obtained in task 4 and using
 613 the proposed method. It is clear that these four parameters
 614 converge after 300 steps, which is as fast as the convergence
 615 speed of reward for task 4 shown in Fig. 10. In order to
 616 test the parameters convergence rate under each method, the

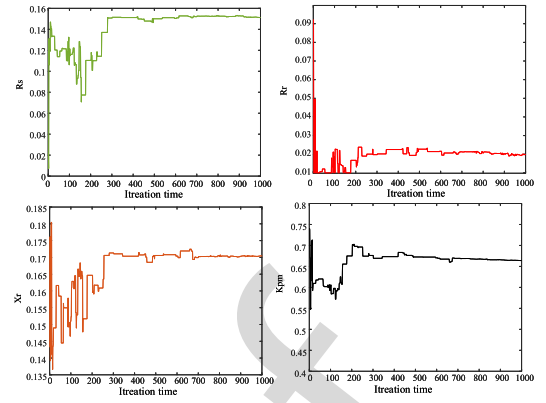


Fig. 14. Parameters convergence rate.

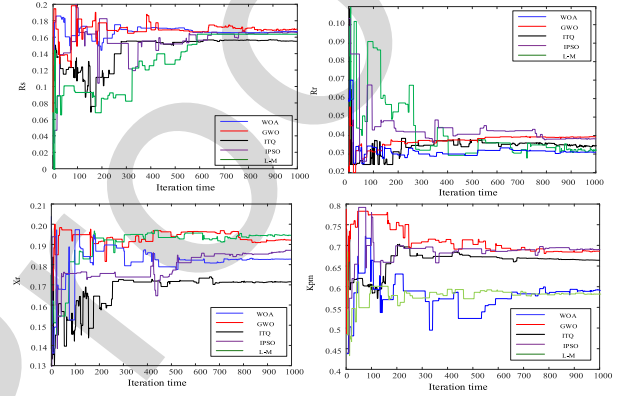


Fig. 15. Comparison of parameters convergence rate.

617 following two figures are provided to show the comparison.
 618 Fig. 15 shows the curve of estimations for four parameters by 5
 619 methods at each iteration step. These methods include: WOA,
 620 GWO, ITQ, IPSO and L-M. The result is based on the data
 621 obtained in task 4 which can be viewed as a new task. Fig. 16
 622 shows statistics of the minimum step for convergence and the
 623 converge criteria requires the relative error to be smaller than
 624 1.5% in 50 consecutive steps. The relative error in n th step σ^n
 625 is defined as:

$$\sigma^n = \left| \frac{X^{n+1} - X^n}{X^n} \right| \quad (20) \quad 626$$

627 where X^n is the estimation is n th step.

628 From the comparisons we can see that our proposed method
 629 achieves a higher accuracy and the parameters estimated
 630 by ITQ can converge in fewer steps, which validates the
 631 effectiveness of the proposed load identification technique.

632 F. Computational Efficiency

633 In order to fully evaluate the efficiency of the proposed
 634 method, Table. V compares the computation time of
 635 optimization process of each method for task 2 and task 3,
 636 which belong to a source task and a new task, respectively.
 637 All the algorithms are implemented in MATLAB R2019a by
 638 a personal computer with Intel(R) i5 CPU at 2.6GHz with
 639 8GB of RAM. Besides, in task 3, the proposed ITQ is able to
 640 transfer optimal knowledge from source tasks.

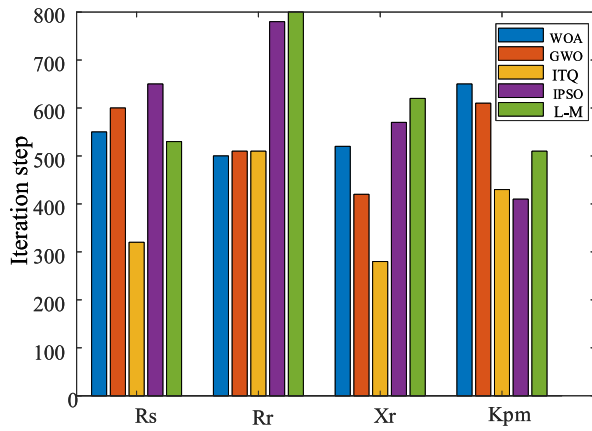


Fig. 16. Minimum iteration step to converge.

TABLE V
COMPARISON OF ESTIMATED PARAMETERS

Method	Task 2		Task 3	
	Number of iterations	Time/s	Number of iterations	Time/s
WOA	332	15.2	-	44.35
GWO	413	14.3	343	11.72
ITQ	292	19.8	8	0.58
IPSO	355	16.3	325	14.51
LM	277	17.52	371	23.92

Note that the computational time required in the optimization of composite load modeling also depends on the number of sampled data. In this study, there are 130 samples in each task. Besides, to offer a fair comparison, the same convergence criteria is used during optimization process. The criteria is for the objective function to reach a value below $1.8e-3$.

From Table. V and Fig. 8, we can see that it takes some time for ITQ agents to solve source task (pre-learning process) by greedy search and guided by teachers (L-M agents). When dealing with a new task, ITQ enables more accurate and efficient parameter identification. In power systems, power companies recorded most measurements during faults and ITQ can complete the pre-learning process by off-line learning based on these previous recorded measurements and identify load parameters in a short time when dealing with a new task.

VI. CONCLUSION AND FUTURE WORK

This article proposes an Imitation and transfer Q-learning based-based composite load parameter identification approach to accelerate the identification rate and improve the identification accuracy. An imitation learning process is introduced to improve the exploitation and exploration process of Q-learning. A transfer learning process is employed to improve the load parameter identification efficiency. Owing to the balance between greedy search and random global search rule, the proposed ITQ can avoid the premature convergence and

search the global optimal result. Simulations on a 68-bus test system have validated the effectiveness of the proposed ITQ method, and the comparisons show that ITQ approach has superior convergence properties owing to the ability to exploit optimal knowledge from source tasks.

Considering the development of complex load models and time-varying load parameters, in the future work, we will extend this approach and explore up-to-date methods to identify the Western Electricity Coordinating Council (WECC) composite load model and time-varying load parameters.

REFERENCES

- A. Arif, Z. Wang, J. Wang, B. Mather, H. Bashualdo, and D. Zhao, "Load modeling—A review," *IEEE Trans. Smart Grid*, vol. 9, no. 6, pp. 5986–5999, Nov. 2018.
- H. Bai, P. Zhang, and V. Ajarapu, "A novel parameter identification approach via hybrid learning for aggregate load modeling," *IEEE Trans. Power Syst.*, vol. 24, no. 3, pp. 1145–1154, Aug. 2009.
- C. Wang, Z. Wang, J. Wang, and D. Zhao, "Robust time-varying parameter identification for composite load modeling," *IEEE Trans. Smart Grid*, vol. 10, no. 1, pp. 967–979, Jan. 2019.
- H. Renmu, M. Jin, and D. J. Hill, "Composite load modeling via measurement approach," *IEEE Trans. Power Syst.*, vol. 21, no. 2, pp. 663–672, May 2006.
- Z. Ma, Z. Wang, Y. Wang, R. Diao, and D. Shi, "Mathematical representation of WECC composite load model," *J. Mod. Power Syst. Clean Energy*, vol. 8, no. 5, pp. 1015–1023, Sep. 2020.
- Q. Huang *et al.*, "Aggregate protection response of motor loads in commercial buildings," in *Proc. IEEE/PES Transm. Distrib. Conf. Exposit. (TD)*, Denver, CO, USA, Apr. 2018, pp. 1–5.
- J. Ma, D. Han, R.-M. He, Z.-Y. Dong, and D. J. Hill, "Reducing identified parameters of measurement-based composite load model," *IEEE Trans. Power Syst.*, vol. 23, no. 1, pp. 76–83, Feb. 2008.
- P. Kundur, N. J. Balu, and M. G. Lauby, *Power System Stability and Control*, vol. 7. New York, NY, USA: McGraw-Hill, 1994.
- J. Zhao, Z. Wang, and J. Wang, "Robust time-varying load modeling for conservation voltage reduction assessment," *IEEE Trans. Smart Grid*, vol. 9, no. 4, pp. 3304–3312, Jul. 2018.
- D. J. Hill, "Nonlinear dynamic load models with recovery for voltage stability studies," *IEEE Trans. Power Syst.*, vol. 8, no. 1, pp. 166–176, Feb. 1993.
- K. Zhang, H. Zhu, and S. Guo, "Dependency analysis and improved parameter estimation for dynamic composite load modeling," *IEEE Trans. Power Syst.*, vol. 32, no. 4, pp. 3287–3297, Jul. 2017.
- D. Han, J. Ma, R. He, and Z. Dong, "A real application of measurement-based load modeling in large-scale power grids and its validation," *IEEE Trans. Power Syst.*, vol. 24, no. 4, pp. 1756–1764, Nov. 2009.
- M. Cui, M. Khodayar, C. Chen, X. Wang, Y. Zhang, and M. E. Khodayar, "Deep learning-based time-varying parameter identification for system-wide load modeling," *IEEE Trans. Smart Grid*, vol. 10, no. 6, pp. 6102–6114, Nov. 2019.
- I. A. Hiskens, "Nonlinear dynamic model evaluation from disturbance measurements," *IEEE Trans. Power Syst.*, vol. 16, no. 4, pp. 702–710, Nov. 2001.
- S. Kamoun and R. Malhamé, "Convergence characteristics of a maximum likelihood load model identification scheme," *Automatica*, vol. 28, no. 5, pp. 885–896, 1992.
- J. De Kock, F. Van Der Merwe, and H. Vermeulen, "Induction motor parameter estimation through an output error technique," *IEEE Trans. Energy Convers.*, vol. 9, no. 1, pp. 69–76, Mar. 1994.
- P. Regulski, D. S. Vilchis-Rodriguez, S. Djurovic, and V. Terzija, "Estimation of composite load model parameters using an improved particle swarm optimization method," *IEEE Trans. Power Del.*, vol. 30, no. 2, pp. 553–560, Apr. 2015.
- R. S. Sutton and A. G. Barto, *Reinforcement Learning: An Introduction (Second Edition)* (Adaptive Computation and Machine Learning). Cambridge, MA, USA: MIT Press, 2018.
- X. S. Zhang, T. Yu, Z. N. Pan, B. Yang, and T. Bao, "Lifelong learning for complementary generation control of interconnected power grids with high-penetration renewables and EVs," *IEEE Trans. Power Syst.*, vol. 33, no. 4, pp. 4097–4110, Jul. 2018.

- 737 [20] L. Yin, L. Zhao, T. Yu, and X. Zhang, "Deep forest reinforcement learn-
738 ing for preventive strategy considering automatic generation control in
739 large-scale interconnected power systems," *Appl. Sci.*, vol. 8, no. 11,
740 p. 2185, 2018.
- 741 [21] S. J. Pan and Q. Yang, "A survey on transfer learning," *IEEE Trans.*
742 *Knowl. Data Eng.*, vol. 22, no. 10, pp. 1345–1359, Oct. 2010.
- 743 [22] L. Xinran, L. Peiqiang, and L. Hui, "Optimized identification strategy
744 for composite load model parameters based on sensitivity and correlation
745 analysis," *Trans. China Electrotechn. Soc.*, vol. 31, no. 16, pp. 181–188,
746 2016.
- 747 [23] T. Eiter and H. Mannila, "Computing discrete fréchet distance," Dept.
748 Inf. Syst., Technische Universität Wien, Vienna, Austria, Rep. CD-TR
749 94/6, 1994.
- 750 [24] S. Mirjalili and J.-S. Dong, *Multi-Objective Optimization Using Artificial*
751 *Intelligence Techniques*. Cham, Switzerland: Springer, 2019.

AQ3



Zhaoyu Wang (Member, IEEE) received the B.S. 781
and M.S. degrees in electrical engineering from 782
Shanghai Jiao Tong University in 2009 and 2012, 783
respectively, and the M.S. and Ph.D. degrees in elec- 784
trical and computer engineering from the Georgia 785
Institute of Technology in 2012 and 2015, respec- 786
tively. He is the Harpole-Pentair Assistant Professor 787
with Iowa State University. His research interests 788
include power distribution systems and microgrids, 789
particularly on their data analytics and optimization. 790
He is the Principal Investigator for a multitude 791
of projects focused on these topics and funded by the National Science 792
Foundation, the Department of Energy, National Laboratories, PSERC, and 793
Iowa Energy Center. He is the Secretary of IEEE Power and Energy Society 794
(PES) Award Subcommittee, the Co-Vice Chair of PES Distribution System 795
Operation and Planning Subcommittee, and the Vice Chair of PES Task Force 796
on Advances in Natural Disaster Mitigation Methods. He is an Editor of IEEE 797
TRANSACTIONS ON POWER SYSTEMS, IEEE TRANSACTIONS ON SMART 798
GRID, IEEE PES Letters, and IEEE OPEN ACCESS JOURNAL OF POWER 799
AND ENERGY, and an Associate Editor of *IET Smart Grid*. 800



Jian Xie (Student Member, IEEE) received the B.S.
and M.S. degrees in electrical engineering from
Southwest Jiaotong University, Chengdu, China, in
2015 and 2018, respectively. He is currently pur-
suing the Ph.D. degree with the Department of
Electrical and Computer Engineering, Iowa State
University, Ames, IA, USA. His research interests
include load modeling and machine learning in
power system monitoring.



Yishen Wang (Member, IEEE) received the B.S. 801
degree in electrical engineering from Tsinghua 802
University, Beijing, China, in 2011, and the M.S. 803
and Ph.D. degrees in electrical engineering from 804
the University of Washington, Seattle, WA, USA, 805
in 2013 and 2017, respectively. He is currently a 806
Power System Research Engineer with GEIRI 807
North America, San Jose, CA, USA. His research 808
interests include power system economics and opera- 809
tion, energy storage, microgrids, load modeling, and 810
PMU data analytics. 811



Zixiao Ma (Graduate Student Member, IEEE) 761
received the B.S. degree in automation and the 762
M.S. degree in control theory and control engi- 763
neering from Northeastern University in 2014 and 764
2017, respectively. He is currently pursuing the 765
Ph.D. degree with the Department of Electrical 766
and Computer Engineering, Iowa State University, 767
Ames, IA, USA. His research interests are focused 768
on the power system load modeling, microgrids, 769
nonlinear control, and model reduction. 770



Ruisheng Diao (Senior Member, IEEE) received the 812
Ph.D. degree in EE from Arizona State University, 813
Tempe, AZ, USA, in 2009. Serving as a Project 814
Manager, PI/co-PI and key technical contributor, 815
he has been managing and supporting a port- 816
folio of research projects in the area of power 817
system modeling, dynamic simulation, online secu- 818
rity assessment and control, dynamic state esti- 819
mation, integration of renewable energy, and HPC 820
implementation in power grid studies. He is cur- 821
rently with GEIRINA as a Deputy Department Head 822
of PMU & System Analytics, in charge of several R&D projects on power 823
grid high-fidelity simulation tools and developing new AI methods for grid 824
operations. 825



Kaveh Dehghanpour (Member, IEEE) received the 771
B.Sc. and M.S. degrees in electrical and computer 772
engineering from the University of Tehran in 2011 773
and 2013, respectively, and the Ph.D. degree in elec- 774
trical engineering from Montana State University in 775
2017. He was a Postdoctoral Research Associate 776
with Iowa State University. His research interests 777
include the applications of machine learning and 778
data-driven techniques in power system monitoring 779
and control. 780



Di Shi (Senior Member, IEEE) received the B.S. 826
degree in electrical engineering from Xi'an Jiaotong 827
University, Xi'an, China, in 2007, and the M.S. 828
and Ph.D. degrees in electrical engineering from 829
Arizona State University, Tempe, AZ, USA, in 2009 830
and 2012, respectively. He currently leads the PMU 831
& System Analytics Group, GEIRI North America, 832
San Jose, CA, USA. His research interests include 833
WAMS, Energy storage systems, and renewable inte- 834
gration. He is an Editor of IEEE TRANSACTIONS 835
ON SMART GRID. 836